ELSEVIER

Seminars in
ROENTGENOLOGY

Sinonasal Neoplasms

Mohit Agarwal, MD,* and Bruno Policeni, MD†

Introduction

If Rip Van Winkle went to medical school during the 80s and woke up today among a meeting of pathologists, he would think he was on a different planet and listening to an alien language. The once "pink and purple" world of pathology is now extensively multicolored with an overwhelming number of immunostains and molecular markers. Histological diagnoses now come with an alphanumeric tail, each implying the unique gene expression associated with that tumor entity. Needless to say, similar things have happened to the new fourth edition WHO classification of sinonasal (SN) neoplasms, where SMARC B1-deficient carcinoma, Nuclear protein testis (NUT) midline carcinoma, and human papilloma virus (HPV)-related multiphenotypic SN carcinoma have found a place.[1]

In the following description of SN neoplasms, we will discuss benign and malignant tumors affecting the nasal cavity and paranasal sinuses, with reference to the new entities included in the latest WHO classification (Tables 1 and 2).[2,3]

Imaging of SN Neoplasms

Imaging differentiation of SN tumors can be difficult. Despite this, it remains a goal of the interpreting radiologist to ascertain if the tumor in question is benign or malignant. Well-defined margins, involvement of a single sinus, homogeneous, low attenuation on CT, and high long TR signal on MR are imaging features suggestive of benignity. Irregular infiltrating margins, bone involvement, extension beyond the sinus walls, high CT attenuation, and hypointense signal on long TR MR sequences are imaging features that raise concern for a malignant process.[4-6] The status of the bone adjacent to the tumor can give useful clues to the nature of the tumor. In general, destructive bone erosion and fragmentation are signs of malignancy, while benign lesions will usually cause bone remodeling and/or sclerosis. Loss of bright fat marrow intensity on T1W MR images is a sign of bone involvement. Differentiation of benign vs malignant lesions remains a challenge with imaging and exceptions to the previously mentioned features exist. Pathology is required to determine the diagnosis in the majority of cases.[7]

Imaging has more to offer than just histological diagnosis, the most important of which is tumor mapping. It must be determined if the tumor is confined within a single sinus or if there is extension into surrounding structures. Tumors of the maxillary sinuses can extend to the anterior ethmoid sinus, nasal cavity, and orbit. Anterior ethmoid tumors can involve the frontal sinuses and the nasal cavity. Nasal cavity tumors commonly involve the ethmoid sinus. Posterior ethmoid tumors tend to involve the sphenoid sinus.[7]

Intracranial extension is a dreaded complication, more commonly seen with ethmoid, sphenoid, and frontal sinus tumors. Images must be carefully evaluated to look for intracranial disease including dural and parenchymal involvement. It may be difficult to confirm dural invasion if the thickening and enhancement is linear. Nodular thickening and enhancement is more indicative of tumor invasion. Abnormal signal/enhancement within the adjacent brain parenchyma is highly suggestive of tumor invasion. A detailed description of bony involvement at the skull base will help in planning the surgical approach and prevent untoward postoperative complications such as cerebrospinal fluid (CSF) leak.

Orbital extension also worsens prognosis and must be identified for optimal treatment planning as orbital exenteration may be necessary.[6] Malignant tumors of the maxillary antrum are most likely to involve the orbits via superior extension. Ethmoid sinus tumors may also extend to the orbits by mere proximity. Posterior ethmoid and sphenoethmoid tumors can invade the orbital apex.

Involvement of the bony palate may alter the surgical course and may herald development of oro-nasal or oro-antral fistulas. Involvement of the pterygopalatine fossa (PPF) is an important imaging finding when mapping SN neoplasms as it is suggestive of perineural tumor spread, an ominous features of SN neoplasms. A rich plexus of nerves traverses the PPF and perineural tumor may extend in an antegrade fashion to involve the peripheral V2 branches or in a retrograde fashion to involve the main trunks of the trigeminal nerve. Even in the

*Department of Radiology, Division of Neuroradiology, Medical College of Wisconsin, Milwaukee, WI.
†Department of Radiology, Division of Neuroradiology, University of Iowa, Iowa City, IA.
Acknowledgments: The authors would like to acknowledge Michelle A. Michel, MD for her contribution of images to this manuscript.
Address reprint requests to Mohit Agarwal MD, 8701 Watertown plank road, Milwaukee, WI 53226. E-mail: magarwal@mcw.edu

 https://doi.org/10.1053/j.ro.2019.03.001

Table 1 WHO Classification of Tumors of the Nasal Cavity, Paranasal Sinuses and Skull Base

Carcinomas
Squamous cell carcinoma
Keratinizing, non-keratinizing and spindle cell
Lymphoepithelial carcinoma
Sinonasal undifferentiated carcinoma
NUT carcinoma
Neuroendocrine carcinomas
Small cell and large cell
Adenocarcinomas
Intestinal-type and non-intestinal type
Teratocarcinosarcoma
Sinonasal papillomas
Inverted, oncocytic and exophytic
Respiratory epithelial lesions
Respiratory epithelial adenomatoid hamartoma (REAH)
Seromucinous hamartoma
Salivary gland tumors
Malignant soft tissue tumors
Fibrosarcoma
Undifferentiated pleomorphic sarcoma
Leiomyosarcoma
Rhabdomyosarcoma
NOS, Embryonal, Alveolar, Pleomorphic, spindle cell
Angiosarcoma
Malignant peripheral nerve sheath tumor
Biphenotypic sinonasal sarcoma
Synovial sarcoma
Borderline/low-grade malignant soft tissue tumors
Benign soft tissue tumors
Leiomyoma
Hemangioma
Schwannoma
Neurofibroma
Other tumors
Meningioma
Sinonasal ameloblastoma
Chondromesenchymal hamartoma
Hematolymphoid tumors
Extranodal NK/T-cell lymphoma
Extraosseus plasmacytoma
Neuroectodermal/melanocytic tumors
Ewing sarcoma/PNET
Olfactory neuroblastoma
Mucosal melanoma

absence of PPF involvement, perineural tumor should be proactively assessed with a thorough inspection of the normal fat pads at the neural foramina and identification of abnormal enhancement along the course of the nerves.

Tumor growth commonly occludes the sinus drainage pathways and a frequent problem during tumor mapping is differentiating tumor from retained secretions within the involved sinuses.[6] Unless inspissated or complicated by hemorrhage or high protein content, retained secretions have a high signal on long TR-weighted images in contrast to hypercellular low signal tumor.

MRI has greater soft tissue distinction compared to CT and remains the modality of choice for accurate tumor mapping and surveillance after treatment.[6,8] Orbital and intracranial tumor extension are more accurately assessed with MRI. Bone destruction, erosion, and remodeling are better assessed on CT, but MRI again proves superior if bone marrow involvement is of concern. MRI is far superior to CT for diagnosing perineural tumor spread. Nodal and distant metastases are best assessed by FDG-PET.[9] With regards to the MRI technique, thin section (3-4 mm) small field of view (FOV) (16-18 mm) short-tau inversion recovery (STIR), precontrast T1W and postcontrast T1W images in at least 2 planes (axial and coronal) provide adequate information in most cases. Use of fat suppression on postcontrast images is necessary to evaluate the abnormal enhancement. A whole-brain FLAIR sequence is optional, but is useful in the evaluation of the brain parenchyma. If used as a supplement to MRI, CT can be performed without contrast to assess bony involvement. If MRI is contraindicated, CT with contrast can be performed for tumor mapping using thin sections (1 mm) and multiplanar reformats.

Quantitative diffusion techniques have been found useful in differentiating benign from malignant tumors, where malignant tumors have lower apparent diffusion coefficient (ADC) values compared to benign processes.[10-16] Diffusion weighted imaging (DWI) and ADC have also been studied to differentiate different tumor types and have revealed overall lower ADC values for lymphomas compared to squamous cell carcinoma (SCC).[10,14] Advanced imaging techniques such as MR perfusion are being investigated for their potential use and encouraging preliminary data have been obtained. Time-intensity curves (TIC) are plotted for dynamic contrast-enhanced MRI to look for maximum (Tmax) and peak enhancement (Tpeak). A "persistent" TIC suggests a benign process, while a "washout" TIC suggests a malignant tumor.[12,17]

Table 2 Emerging Sinonasal Neoplasms

SMARCB1 (INI-1) deficient sinonasal carcinoma
HPV-related sinonasal carcinoma
HPV-related multiphenotypic sinonasal carcinoma
Renal cell-like adenocarcinoma

Clinical Features

Approximately 3% of head and neck malignancies arise in the SN region.[6] This compromises 0.2%-0.8% of all malignancies,[6] a low number. Despite their rare occurrence, they are clinically significant due to the grim prognosis. By the time of presentation, the tumors are typically advanced, further complicating the treatment in an anatomic location fraught with concerns of postoperative dysfunction and cosmesis. Symptoms are usually vague and overlap with those of sinusitis and dental infection. Common symptoms including nasal stuffiness, headache, and vague orbital pain may not always prompt an imaging investigation, further delaying diagnosis. Obvious signs of a mass such as proptosis, epistaxis, or facial deformity suggest advanced disease. Symptoms of trigeminal neuralgia and facial paralysis raise concern for perineural tumor spread.

Types of SN Neoplasms

The histological diversity of SN neoplasms is surprising considering that the apparent contents within the cavities are air and a thin mucosal lining. This region has one of the widest latitude of potential tumor types among the head and neck sites. The tumors can be of epithelial, mesenchymal, lymphoid, or melanocytic origin. The epithelial and mesenchymal tumors can be benign or malignant. Lymphoid and melanocytic tumors in the SN region are usually malignant. Table 1 outlines the 2017 fourth edition WHO classification of the tumors of the nasal cavity and paranasal sinuses. Four new entities are included in the WHO classification, 2 benign and 2 malignant.[1-3] New benign lesions include seromucinous hamartoma and chondromesenchymal hamartoma (CMH).[18] New malignancies are the NUT carcinoma and the biphenotypic SN sarcoma (BSNS). Several emerging entities have also been described and are listed in Table 2. Of note, a number of entities have been removed from the new classification including all benign bone and cartilage tumors, chondrosarcoma, osteosarcoma, chordoma, and diffuse large B-cell lymphoma (DLBCL) among various others.

Malignant tumors of the SN cavities are more common than benign tumors (if incidental osteomas are excluded), and SCC is by far the most common malignancy.[4-8] The most common site of malignancy is the maxillary antrum, although adenocarcinomas have a predilection for the ethmoid sinuses. Papillomas are the most common benign tumors.

Benign Tumors

Papillomas

Papillomas comprise 0.4%-5% of the SN tumors and arise from the mucosal lining, termed the Schneiderian mucosa.[6] Three types are described including, the inverted, the oncocytic, and the exophytic (fungiform). The most common are the exophytic or fungiform papillomas (50%), followed by inverted papillomas (IPs) and lastly the oncocytic papillomas which are rare.

Exophytic papillomas occur in the third to sixth decades of life and are much more common in males. They usually arise in the lower anterior nasal septum and rarely, if ever, undergo malignant transformation. Oncocytic papillomas are rare and occur in individuals beyond the sixth decade with no sex predilection. Like the IP, oncocytic papillomas are most frequent along the lateral nasal wall. A total of 10% are reported to undergo malignant transformation.[6,19]

IPs are more common in the fourth to sixth decades and have a 3:1 male preponderance. The characteristic site of origin is along the lateral nasal wall near the middle meatus.[19,20] The maxillary and ethmoid sinuses may be secondarily involved. Isolated involvement of a sinus without involvement of the nasal cavity is rare. HPV DNA has been isolated in approximately one-third of IPs and approximately two-thirds of IPs with associated squamous carcinoma. Malignant transformation associated with IP may be coexistent or develop later and is seen in approximately 10% of cases.[19,20] On imaging, IP presents as an expansile SN mass with remodeling and displacement of the surrounding bony structures. Areas of calcification may be seen on CT. A focal area of hyperostosis may be seen, which represents the site of attachment of the tumor (Fig. 1). This bony strut is important to be reported in order to achieve complete resection.[20] A convoluted, "cerebriform" appearance on long TR and postcontrast T1W MR images is highly predictive of IP.[6,19,20] Findings of necrosis, loss of the cerebriform architecture, and bone destruction should alert the radiologist to the presence of malignancy. Lateral rhinotomy with en bloc resection of the mass and the bony point of attachment is the treatment of choice due to the high rate of recurrence. Smaller lesions can be approached with more conservative, endoscopic techniques and followed with close clinical and imaging surveillance, but this remains controversial.

Fibro-osseous Lesions

Fibro-osseous lesions are a diverse group of benign lesions that have similar histopathological features and may be difficult to differentiate. Imaging features, particularly on MRI can be highly variable making diagnosis difficult. CT can often add useful information in differentiation. Osteoma, ossifying fibroma, and fibrous dysplasia (FD) are the most common lesions in this category. Imaging aids in determining the extent of lesions that may require surgical intervention including

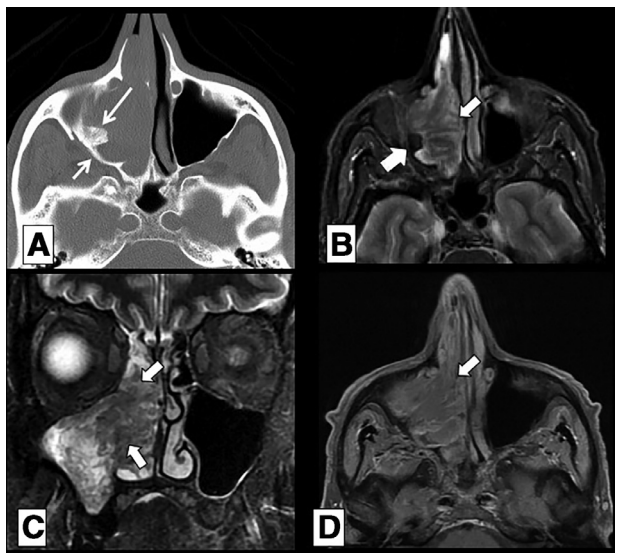

Figure 1 Inverted papilloma. Axial noncontrast CT in bone algorithm (A) shows an expansile mass within the right maxillary sinus extending into the nasal cavity and widening the right maxillary infundibulum. There is thickening of the maxillary sinus walls (short thin arrow) indicative of chronic inflammation. A focal area of bony hyperostosis (long thin arrow) represents the site of attachment of the tumor and is important to report to achieve complete resection. Axial (B) and coronal (C) STIR MRI images show hyperintense appearance of the mass with the characteristic convoluted "cerebriform" architecture (small block arrows in B and C). Hypointense site of bony attachment (thick block arrow) is seen in B. Diffuse enhancement is seen in the axial postcontrast fat suppressed T1W MRI image (D) with the characteristic cerebriform architecture (small block arrow).

those producing significant cosmetic deformity, orbital compromise, and sinus obstruction.

Osteomas are the most common fibro-osseous lesions and also the most common benign SN tumors.[21,22] Frontal and ethmoid sinuses are the most frequently affected. They are sharply marginated and have a broad base along the bony sinus wall, although they may have a short pedicle. They are usually homogenous and demonstrate a dense osseous appearance that is hypointense on all MR sequences (Fig. 2). Occasionally, internal fibrous components may be present which are hyperintense on long TR images and enhance on contrast administration.

Ossifying fibromas are most common in between 10 and 40 years and have a female predilection.[21-24] They continue to grow after skeletal maturation ceases and demonstrate progressive proliferation and bone expansion. On imaging, these lesions are well-circumscribed round or ovoid lesions often with sclerotic margins and a low attenuation fibrous center on CT.[21-24] The fibrous center may enhance with contrast.

FD is a fibro-osseous lesion in which medullary bone is replaced by immature tissue of varying fibrous and osseous components. FD presents in the first 2 decades of life and may continue to progress until skeletal maturation. FD does not respect suture lines and may involve multiple bones (Fig. 3). FD appears as an expansile lesion, classically with a "ground-glass" matrix and with thinning of the overlying cortex. The appearance depends on the amount of osseous and fibrous tissue. Lesions with predominantly fibrous tissue are hyperintense on long TR images and enhance, which may mimic neoplasm (Fig. 3). Correlation with CT can help in these difficult cases.[20-23]

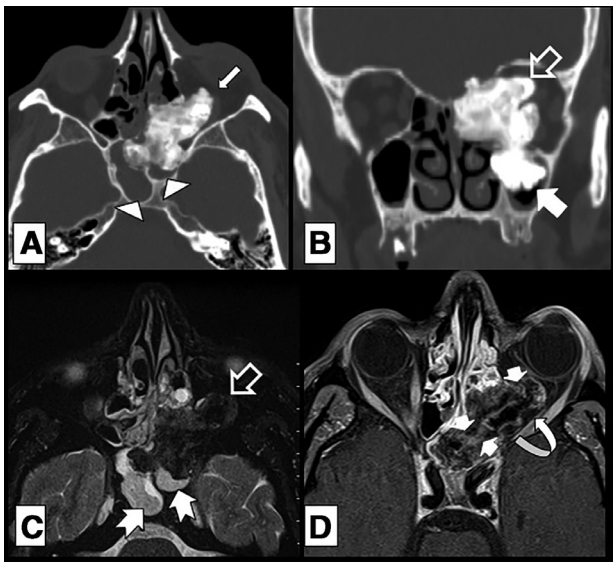

Figure 2 Osteoma. Axial (A) and coronal (B) bone algorithm CT images show a large lobulated osteoma within the left posterior ethmoid extending into the left orbit (thick arrow in A and open arrow in B) and bilateral sphenoid sinuses. Opacification of the sphenoid sinuses (arrowheads in A) is due to the obstruction of the sphenoid ostia and retained secretions. The osteoma also extends into the left maxillary sinus (solid arrow in B). In spite of the multispatial extension, sharp margins, and the classic densely ossified appearance suggests the benign nature. Axial STIR MRI (C) shows profound hypointensity within the mass (open arrow) due to the dense osseous components. Retained secretions are seen in the sphenoid sinuses (notched arrows). Axial post contrast fat suppressed T1W MR image (D) shows the large osteoma with intraorbital extension (curved arrow). Areas of enhancement (small block arrows) represent the fibrous component of the lesion.

Benign Soft Tissue Neoplasms

The 3 benign soft tissue lesions that we will discuss here are leiomyoma, juvenile angiofibroma, and schwannoma.

Leiomyomas

Leiomyomas are benign tumors with smooth muscle differentiation and are rare in the SN region. They are more common in the nasal cavity than in the paranasal sinuses. They are more common in adults and there is no sex predilection. On imaging, leiomyomas are homogeneous expansile masses isodense to other soft tissue on CT and are slightly hyperintense on long TR MR images. Moderate contrast enhancement is seen. There may be bony remodeling without erosion.[6,19,25,26]

Schwannomas

Schwannomas are slow growing benign tumors arising from spindle cells of the nerve sheath and are most common in the ethmoid sinuses followed by the maxillary sinus and the nasal cavity. On CT, these tumors present as hypodense soft tissue masses with surrounding bone remodeling. On MRI,

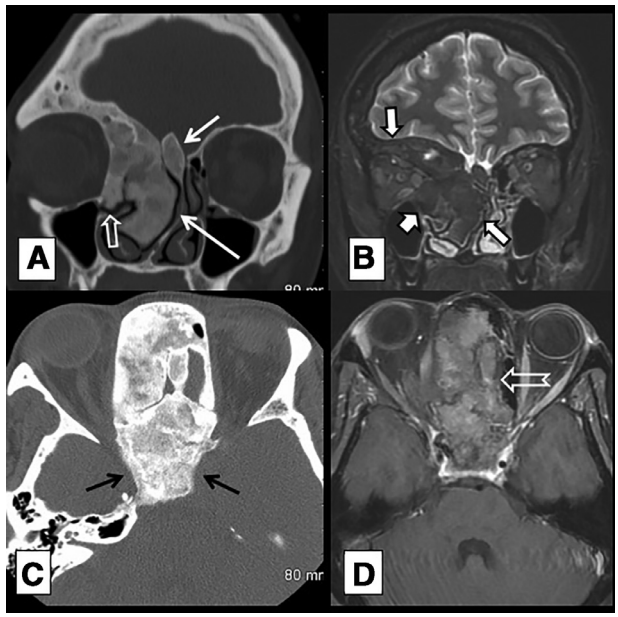

Figure 3 Fibrous dysplasia. Coronal (A) and axial (C) bone algorithm CT images through the face show a large fibrous dysplasia involving the right orbital roof and medial wall, the right middle turbinate (long thin arrow in A), and the crista galli (short thin arrow in A). Distortion of the right maxillary ostium is noted (open arrow in A). Extensive sphenoid body involvement is also noted (black arrows in C). Diffusely hypointense appearance is noted on coronal STIR MRI image (B) marked by block arrows. Contrast enhancement is not uncommon in fibrous dysplasia and represents the fibrous component, marked by notched open arrow in the axial postcontrast fat suppressed T1W MRI image (D). Involvement of multiple adjacent bones across suture lines is typical.

the lesions are hypointense on T1W and hyperintense on long TR images, although SN schwannomas may be less hyperintense than those in other parts of the body due to high ratio of hypercellular Antoni A cells (Fig. 4). There is moderate enhancement on contrast administration and sometimes a "target" appearance may be seen. Frequently, cystic and hemorrhagic components are present.[6,19,25,26]

Juvenile Angiofibroma

Juvenile angiofibroma is a highly vascular benign soft tissue tumor which deserves special mention. It typically occurs in young males in the second decade presenting with epistaxis and unilateral nasal obstruction. The lesions arise in the sphenopalatine foramen and grow medially into the nasal cavity, laterally into the PPF and posteriorly into the nasopharynx.[20] Biopsy of these lesions can be catastrophic due to the highly vascular nature.

On imaging, these lesions are of soft tissue attenuation on CT. On MRI, they are hypointense on T1W and hyperintense on T2W images. Intense postcontrast enhancement is seen with frequent low intensity areas representing flow voids within the vessels. Catheter angiography can be used for tumor mapping and for preoperative embolization to minimize blood loss during surgery.[20]

SN Pleomorphic Adenoma

SN pleomorphic adenomas are rare and most arise from the nasal septum, followed by lateral nasal wall and maxillary sinus in decreasing order of frequency. These tumors are smoothly marginated and cause remodeling of the adjacent bone. The high T2W signal commonly seen in pleomorphic adenomas of the major salivary glands may not always be seen here as these tumors are commonly more cellular making them to appear of intermediate signal on T2W images.[6,19,20] Aggressive features such as bone destruction and heterogeneous appearance are concerning for malignant conversion known as carcinoma-ex-pleomorphic adenoma, in which case they are difficult to differentiate from SCCs.

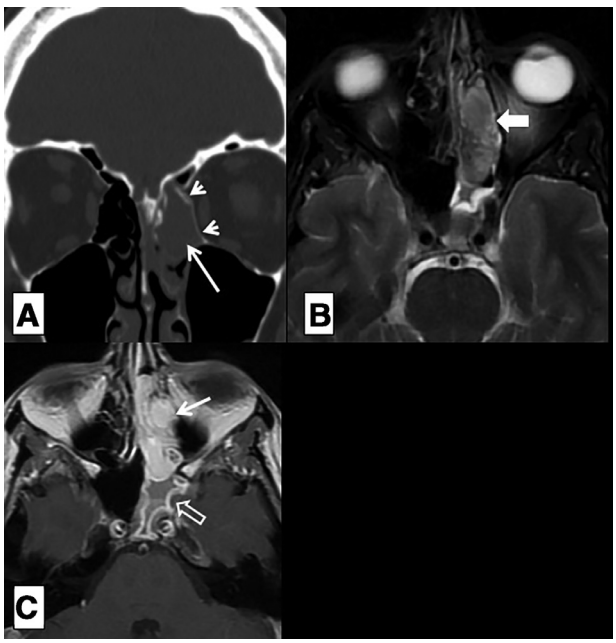

Figure 4 Nasal cavity schwannoma. Coronal bone algorithm CT (A) image shows a homogenous expansile soft tissue lesion in the superior left nasal cavity (long thin arrow). There is remodeling of the adjacent bone (arrowheads). Axial STIR MRI image (B) shows a well-defined lesion with smooth margins and intermediate T2 signal (solid arrow). Postcontrast fat suppressed axial image (C) shows an avidly and uniformly enhancing mass (thin arrow). Retained secretions are seen in the left sphenoid sinus (open arrow).

Malignant Tumors

Squamous Cell Carcinoma

SCC is by far the most common SN neoplasm and arises most frequently in the maxillary sinus. The other sites in order of occurrence are the nasal cavity and the ethmoid complex, frontal sinus, and sphenoid sinus. Various histological appearances include the keratinizing, nonkeratinizing, and spindle cell types. Exposure to nickel, wood dust, chromium, and other substances have been found to increase the risk of developing these tumors with a latency period of up to 20-30 years. SCC may also arise in IPs. A history of chronic sinusitis has also been associated with increased SCC risk, although a causal relationship of this is uncertain.[27,28] Males between the ages of 55 and 65 years are most commonly affected.[4,5,7,8,13,20,23]

Imaging features are nonspecific and general imaging features of invasiveness are taken as signs of malignancy. CT can help identify bone erosion. Loss of thin low signal intensity of the bone cortex and infiltration of high signal intensity marrow fat on T1W images are useful signs on MR to identify bone involvement. It is important to assess for breach of the periorbita as significant orbital involvement has direct management implications. Examination of the bone and periosteum of the pterygoid plates and examination of fat within the PPF can help identify involvement of this region and to detect subtle or early perineural tumor (Fig. 5). Intracranial extension and involvement of the orbital apex indicate the highest T- stage (T4).[6] Intracranial extension is best assessed by contrast-enhanced MRI. Cribriform plate erosion, visible tumor in the anterior or middle cranial fossa, nodular dural enhancement, and frank brain involvement are ominous signs. Nodal involvement and distant metastatic disease are uncommon even in the presence of advanced local disease. Surgery and radiotherapy are the preferred treatments and local recurrence is the main cause of treatment failure.[4,5,7,8,13,20,23]

Adenocarcinoma

Adenocarcinomas comprise approximately 10% of all SN neoplasms and can be histologically subclassified into intestinal-type adenocarcinomas (ITAC) and nonintestinal type (non-ITAC). This distinction is important due to the high-risk association of exposure to hardwood dust and chemicals used in the leather industry with ITAC development. Males between 55 and 60 years of age are exceedingly more commonly affected than other demographic groups. These tumors,

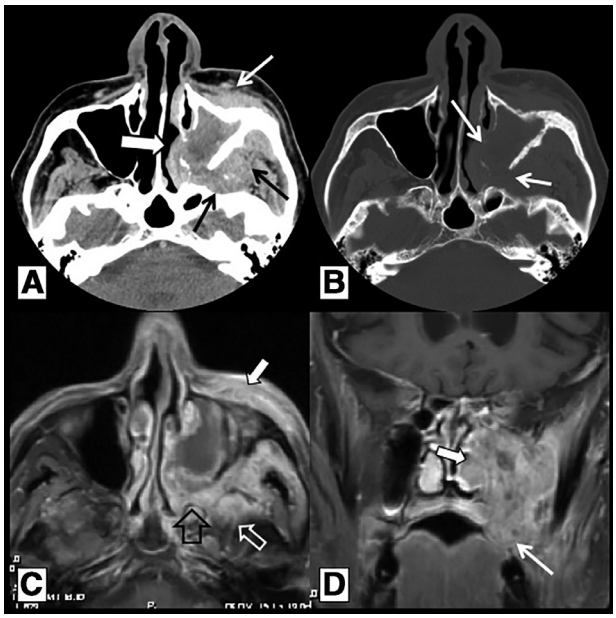

Figure 5 Maxillary sinus squamous cell carcinoma. Axial postcontrast soft tissue CT image (A) shows a large destructive mass in the left maxillary sinus with extension into the nasal cavity (thick arrow). Lobulated mass is noted in the premaxillary region indicative of facial soft tissue involvement (white thin arrow). Thickening and smudging of soft tissues in the masticator space (black thin arrows) also suggests involvement. Axial bone algorithm CT image (B) shows destruction of the medial (long thin arrow) and the posteromedial (short thin arrow) maxillary walls. Axial postcontrast fat suppressed T1W MRI image (C) better delineates the facial soft tissue (thick arrow) and masticator space (white open arrow) extension. Enhancing mass is seen in the pterygopalatine fossa (PPF) marked by black open arrow. Involvement of PPF should alert the radiologist and initiate the search for perineural tumor spread. Multiplanar imaging is essential for complete tumor mapping. Note the extension of tumor into the oral cavity on coronal postcontrast fat suppressed T1W MRI image (D) marked by thin arrow. Nasal cavity extension and involvement of the middle and inferior turbinates is also better appreciated on the coronal image (thick arrow).

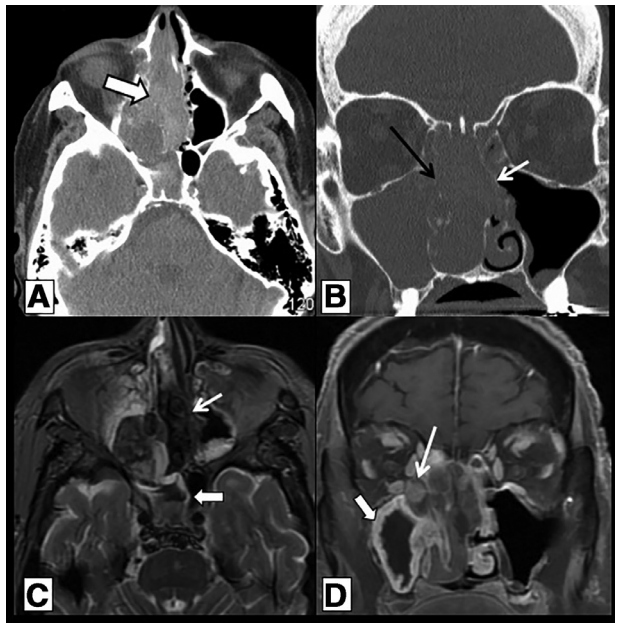

Figure 6 Intestinal-type adenocarcinoma (ITAC). Axial soft tissue CT image (A) shows a heterogeneous expansile destructive mass centered within the ethmoids (thick arrow). ITACs have a predilection for ethmoid sinuses. Coronal bone algorithm CT image (B) shows the mass filling the ethmoids and the right nasal cavity with destruction of the ethmoid air cells, nasal septum and the right-sided turbinates (black arrow). There is extension into the left nasal cavity and displacement of the left lateral nasal wall is seen (white thin arrow). Axial STIR MRI (C) image shows a heterogeneous mass in the ethmoids. T2 low intensity areas (thin arrow) could represent areas of high cellularity or hemorrhage. Distinction of retained secretions (thick arrow) from tumor is better on MRI. Coronal postcontrast T1W MRI image (D) shows a destructive mass with large areas of necrosis represented by areas of nonenhancement. Extension into the left orbit is seen (thin arrow). Low intensity retained secretions and thin linear mucosal enhancement are seen in the right maxillary sinus (thick arrow) helpful in mapping the true extent of the tumor.

especially those associated with occupational exposure, have a predilection for the ethmoid sinuses (Fig. 6).[4,5,7,8,20,23]

The non-ITAC tumors can be low or high grade. The high-grade nonITACs are histologically heterogeneous and likely represent a collection of several different adenocarcinoma subtypes. Low-grade adenocarcinomas have an excellent prognosis and histologically have a tubulo-glandular or papillary architecture. A distinct entity called the SN renal cell-like adenocarcinoma has been recognized in this group which may histologically resemble metastatic renal cell carcinoma (RCC). This distinct tumor will be described later in the new/emerging entities section. Non-ITACs occur more commonly in the maxillary sinuses. Involvement of the nasal cavity and ethmoid sinuses is likely to produce symptoms earlier in the disease course and the non-ITAC types tend to be detected at a less advanced stage.[4-8,20,23]

From an imaging standpoint, adenocarcinomas are indistinguishable from SCC, although frequent ethmoid sinus location can be used as a differentiating feature. SCCs also tend to enhance less avidly compared to adenocarcinomas.[20] The primary role of imaging remains tumor mapping, assessment of local tumor spread and detection of distant metastasis.

Adenoid Cystic Carcinoma

Adenoid cystic carcinomas (ACCs) arise from minor salivary glands and are the most common salivary gland neoplasms in the SN cavities. They account for 5%-15% on SN tumors. In the order of decreasing frequency, they arise in the maxillary antrum, nasal cavity, ethmoid sinus, sphenoid sinus and least commonly, the frontal sinus. ACC also commonly invades the nasal cavity and adjacent sinuses by direct extension from a primary palate lesion. All age ranges can be affected by this tumor although the peak incidence is between 30 and 60 years. These tumors are slow growing but locally aggressive and have the highest rate of local recurrence among the SN tumors.[4-8,20,23] ACCs have a high propensity for perineural tumor spread (Fig. 7), which increases the likelihood of recurrence due to the presence of "skip lesions." Uninvolved nerve segments are

punctuated by areas of perineural tumor and falsely negative tumor margins at surgery can lead to tumor recurrence.[29,30] Distant metastases are not uncommon and may involve the lungs, brain, and bone. Imaging features are nonspecific and resemble that of any aggressive tumor. Perineural tumor spread is important to identify and the interpreting radiologist should bear in mind that skip lesions may be present, warranting examination of the entire course of the nerve.[31] Wide local excision is the treatment of choice and postoperative radiation reduces the chances of recurrence.

Salivary Gland Tumors Other Than ACC

Mucoepidermoid carcinoma, pleomorphic adenoma (benign mixed tumor), and salivary-type adenocarcinoma are less common tumors of salivary gland origin. Pleomorphic adenomas have been described above under the benign tumors section. Salivary-type adenocarcinoma and mucoepidermoid carcinoma arise in the maxillary sinus and nasal cavity. Most of these neoplasms are intermediate or high grade, warranting surgical excision with negative margins. Imaging appearance depends on the tumor grade with the high-grade tumors presenting with aggressive features of bone destruction and adjacent space invasion.

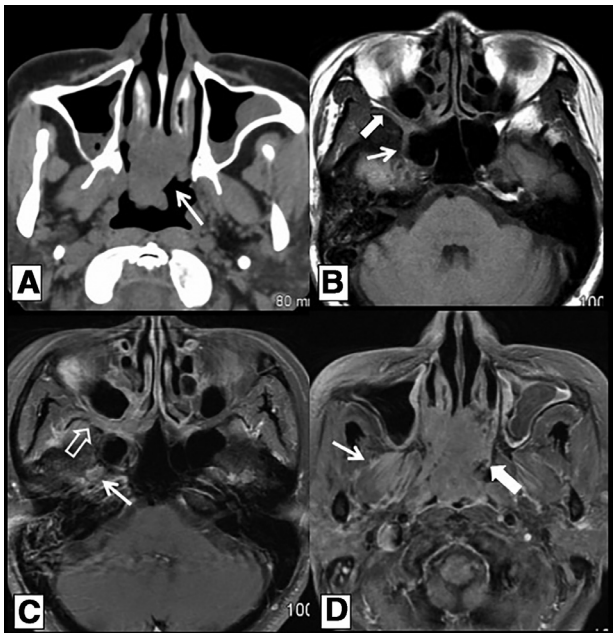

Figure 7 Adenoid cystic carcinoma (ACC). Axial soft tissue CT image (A) shows a lobulated mass in the posterior nasal cavity and nasopharynx (thin arrow). Axial precontrast T1W MRI image (B) shows infiltration of the right PPF (thick arrow) and soft tissue within the right foramen rotundum (thin arrow) indicative of perineural tumor spread (PNTS). ACCs have a high incidence of PNTS. Enhancing soft tissue is noted within the right PPF on axial postcontrast T1W MRI image (C) marked by the open arrow suggestive of PNTS. PNTS is also noted along the right foramen ovale (thin arrow) suggested by its widening and asymmetric contrast enhancement. Enhancement of the right-sided muscles of mastication indicative of denervation injury, marked by thin arrow in D (axial post contrast T1W image). Avidly enhancing mass in the posterior nasal cavity and nasopharynx is redemonstrated (thick arrow).

Esthesioneuroblastoma (Olfactory Neuroblastoma)

Esthesioneuroblastoma (ENB) is a malignant neuroectodermal tumor arising from the olfactory mucosa in the superior nasal cavity. Overall, they comprise approximately 5% of the SN neoplasms. ENB has a bimodal age distribution and peaks in the second and sixth decades.[6,7,20] Males are slightly more commonly affected than females. Histologically, varying degrees of differentiation are seen. On imaging, ENBs present as unilateral or bilateral superior nasal cavity masses with frequent involvement of the ethmoid and sphenoid sinuses by direct extension. Depending on the degree of differentiation, low-grade tumors are seen to remodel the adjacent bone while bone erosion can be seen with higher grade tumors. Intratumoral calcification on CT is not uncommon. On MRI, these tumors are of intermediate signal intensity on T1W images and are slightly hyperintense on T2W images. Avid homogeneous enhancement is seen with frequent intraorbital and intracranial extension. Intracranial extension can be purely extra-axial but may involve the brain parenchyma as well. In the latter case, presence of peritumoral cysts at the tumor-brain interface are highly suggestive of ENB[20] (Fig. 8).

From a tumor mapping perspective, assessment is made whether the tumor is purely intranasal, whether it involves one or more sinuses or whether it extends beyond the nasal cavity and paranasal sinuses; each of these distinctions classifying the tumor to Kadish A, B, and C stages, respectively.[6] To this end, assessment of intraorbital, intracranial, and intracerebral involvement is also valuable since such differentiation alters management. Five-year survival rates range from 80% to 40% depending on histological grade.[4-8] Regional lymphadenopathy is seen in approximately a quarter of cases and distant metastasis is seen in approximately 38%. Delayed recurrence is known to occur with latency of up to 20 years.[6]

SN Neuroendocrine Carcinoma

The historically referred carcinoids in this category of SN tumors have not been specifically addressed in the new WHO classification. In the new edition, SN neuroendocrine carcinomas (SNECs) are separated into small and large cell types (Table 1), similar to their counterparts seen in the lung. Neuroendocrine features may be seen in a number of tumors including ENB, SNEC, NUT carcinoma, and SN undifferentiated carcinoma (SNUC); with ENB representing the most differentiated end of the spectrum and SNUC representing the least differentiated end.[32] SNECs are high-grade tumors usually seen in middle and older age, more frequent in males. Imaging features resemble those of a highly malignant tumor with necrosis and bone destruction (Fig. 9). Early metastasis and local recurrence are common.

SN Undifferentiated Carcinoma

This entity represents undifferentiated SN tumors without definite glandular or squamous features, and thus remains a diagnosis of exclusion. Immunohistochemistry and genetic

Figure 8 Esthesioneuroblastoma. Axial soft tissue CT image (A) shows a destructive mass in the right superior nasal cavity and ethmoids (thin black arrow) extending into the right orbit (thick white arrow). Coronal bone CT (B) shows destruction of the anterior skull base (thick white arrow) and the medial right orbital wall (small thin white arrow). There is inferior extension into the nasal cavity with destruction of the right-sided turbinates and bony structures at the right maxillary ostium (long thin black arrow). Areas of calcification are seen within the intracranial component of the tumor (small thin black arrow). Axial STIR MRI image (C) shows low intensity areas within the tumor indicative of areas of calcification (open arrow). Cystic areas are seen at the margin of the tumor at the tumor-brain interface (thin white arrows). Sagittal postcontrast T1W MRI image (D) shows the avidly enhancing nasal mass extending into the anterior cranial fossa (open arrow) with a cystic area at the tumor margin (thin arrow). Cystic areas at the tumor-brain interface are highly suggestive of esthesioneuroblastoma.

sequencing have found several subsets of tumors in this category with some showing IDH2 mutations at R172 and some showing a complete loss of SMARCB1 expression due to a homozygous deletion – an emerging entity known as SMARCB1(INI1) deficient SN carcinoma.[18,33] It is suggested that other genetically defined entities may be present within the spectrum of SNUC, that may in the future be excluded from this umbrella diagnosis. Imaging features of SNUCs are similar to those of SCCs or SNECs although these tumors are much more aggressive with frequent areas of tumor necrosis. Distant and nodal metastases are more common in SNUCs compared to other SN malignancies (Fig. 10).

SN Melanoma

SN malignant melanomas are rare and are derived from the melanocytes migrated from the neural crest. They develop between 50 and 70 years of age and mostly arise in the nasal cavity. Less commonly, they may arise in the sinuses, of which maxillary sinus is the most common site. Presence of paramagnetic melanin within these tumors gives rise to the

Figure 9 Sinonasal neuroendocrine carcinoma (SNEC). Axial bone CT image (A) shows a lobulated mass in the left nasal cavity (open arrow) with destruction of the left lateral nasal wall (thin white arrow) and the left inferior turbinate. Coronal postcontrast T1W MRI image shows the avidly enhancing mass in the left nasal cavity (thick black arrows) obstructing the left maxillary ostium. Retained secretions and thin mucosal enhancement is noted in the left maxillary sinus (thin black arrow) and in the left ethmoid air cells (thin white arrow). MRI is far superior in delineating tumor extent and in differentiating retained secretions and mucosal disease from tumor, while CT is better at the assessment of cortical bone changes.

characteristic MR T1W hyperintensity (Fig. 11); however, an intermediate signal intensity on T1W images is not uncommon if melanin content is low. Homogeneous intense contrast enhancement is seen on CT and MRI due to rich tumor vascularity.[5,7,8,20] It is important to know that malignant melanomas may commonly masquerade a benign lesion by causing bone remodeling rather than frank bone destruction, and by demonstrating a noninvasive bland margin. In the case of melanomas, these features should not be mistaken for a low-grade lesion.[6]

Wide local excision is the treatment of choice. A total of 40% tumors present with lymphadenopathy. Distant metastatic disease and perineural tumor spread are common. A total of 65% patients may have recurrence.[5,7,8]

SN Lymphoma

SN lymphomas (SNLs) can be classified as B-cell or T-cell (T/NK-cell or T/null-cell). The DLBCL have been excluded from the current WHO classification of nasal cavity and SN tumors since it was determined that the histologic features of DLBCL are sufficiently well described in other parts of the book and duplication served no useful purpose. The extranodal T/NK-cell lymphoma has a specific predilection for the SN tract and has therefore specifically been included in the SN chapter. Any type of lymphoma may however be present in the SN region.

The B-cell and T-cell lymphomas are distinct on several accounts. B-cell SNL (DLBCL phenotype) is more common in Western countries while the T-cell (the more common T/NK-cell phenotype) is more common in Asians. There is strong association of T/NK-cell with Epstein-Barr virus while B-cell SNL is Epstein-Barr virus-negative. B-cell SNL is more common in the sinuses and demonstrates more frequent orbital involvement compared to T/NK-cell SNL. T/NK-cell SNL affects relatively younger individuals and

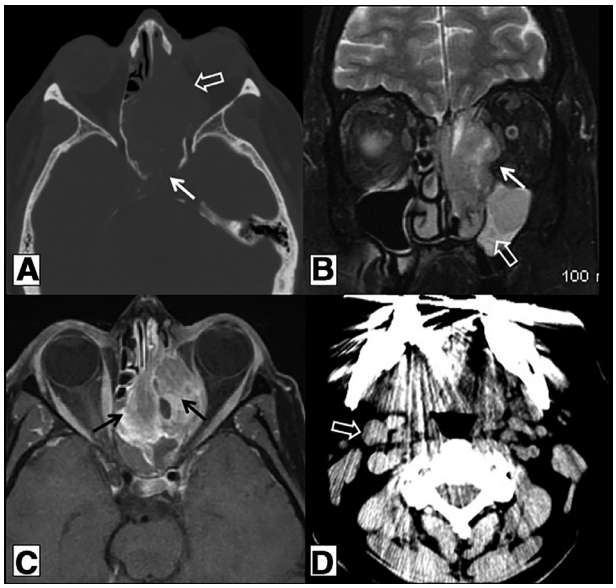

Figure 10 Sinonasal undifferentiated carcinoma (SNUC). Axial bone CT image (A) shows a large aggressive mass centered in the nasal cavity and ethmoid with destruction of the bony structures and extension into the left orbit (open arrow). There is extension into the sphenoid sinuses with erosion of the posterior sphenoid sinus wall (thin white arrow). Coronal STIR MRI (B) shows predominantly intermediate signal mass in the nasal cavity and ethmoids with orbital invasion (thin white arrow). Retained secretions in the left maxillary sinus due to ostium obstruction (open arrow). Axial postcontrast T1W MRI shows avidly enhancing mass with areas of necrosis extending across the midline and invading the left orbit (thin black arrows). Enlarged metastatic right level IIA lymph node is seen (open arrow) on noncontrast axial soft tissue CT image obtained for PET/CT (D). SNUCs are highly aggressive tumors with a high rate of nodal involvement and distant metastasis. NUT gene status is unknown in this case. Aggressive sinonasal tumors with nodal involvement, distant metastasis, and undifferentiated histological component should now be tested for NUT rearrangement.

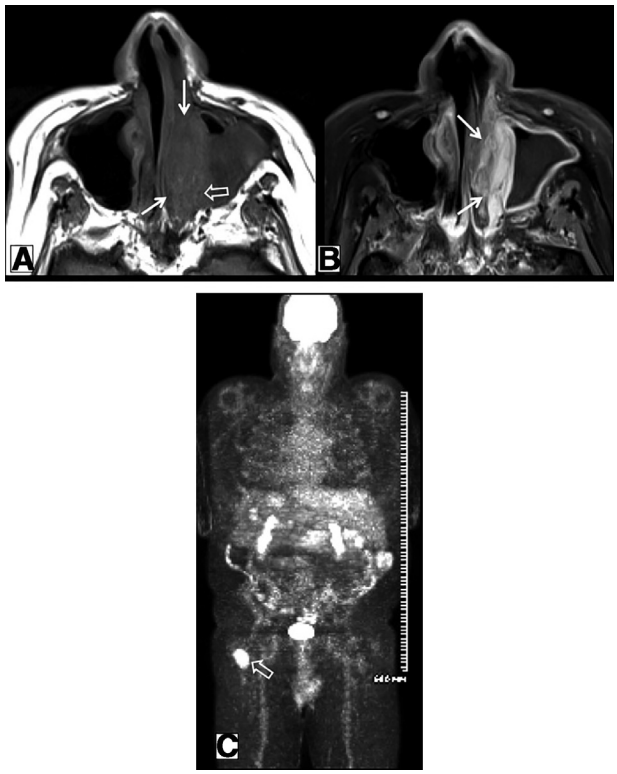

Figure 11 Sinonasal melanoma. Axial precontrast T1W MRI image (A) shows a lobulated left nasal cavity mass (thin white arrows). The mass contains T1W hyperintense components (open arrow), indicative of paramagnetic melanin. Axial postcontrast T1W image (B) shows diffuse enhancement (thin white arrows). Coronal FDG-PET image (C) shows a metastatic lesion within the right femur (open arrow).

typically arises in the nasal cavity presenting with more aggressive imaging features including an angio-invasive pattern, and frequently involves multiple extranodal sites. On imaging, SNLs present as bulky homogeneous soft tissue masses with moderate enhancement. Mild hyperattenuation on CT and low signal intensity on T2W MRI could be due to cellular nature of the tumor. The cellular nature of the tumor is the likely cause for frequent restricted diffusion and low ADC values (Fig. 12). Lobulated homogeneous bulky appearance and low ADC values can be used as imaging features to differentiate SNLs from SN SCC.[6-8,10,11,15,17] SNLs are treated with chemoradiation.

Sarcomas

A lot of sarcomas have been removed from the new WHO classification, including osteosarcoma and chondrosarcoma, since it was felt that these have been described sufficiently in other parts of the WHO classification book. The entities that have been retained are the various types of rhabdomyosarcomas, fibrosarcoma, angiosarcoma, leiomyosarcoma, and synovial sarcoma. This group also includes a new entity called the BSNS, which will be described in the new/emerging entities section.

Rhabdomyosarcomas are childhood tumors with peak incidence between 2 and 5 years and are the most common soft tissue sarcomas in children. Orbit is the most common subsite in the head and neck followed by nasopharynx, middle ear, and SN cavities, in decreasing order. On imaging, these tumors are homogeneous and show moderate enhancement. Both bone remodeling and bone destruction may be seen. Signal intensity is intermediate on all MR imaging sequences. Lymph node involvement is common and distant metastasis can occur.[4-6,25]

Head and neck osteosarcomas are most common in the jaws and maxillary involvement being more common than the mandible. The incidence peaks in the third decade. Predisposing conditions include Paget's disease and FD. Imaging shows the typical “sunburst” periosteal reaction and focal bone destruction. On MR, the tumor is low signal intensity on T1W images and intermediate on T2W images. Moderate contrast enhancement is seen.[20,23]

Head and neck chondrosarcomas are rare and can occur secondary to radiation or due to predisposing conditions such as Maffucci and Ollier syndromes. Maxillary alveolus, maxillary sinus, and nasal septum are the common sites of

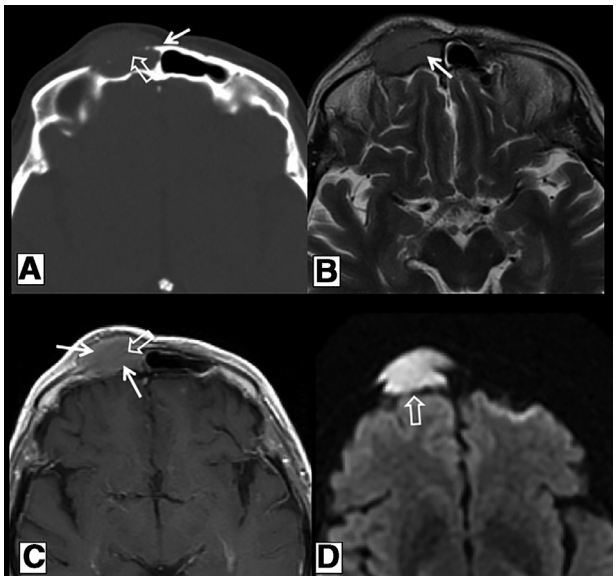

Figure 12 B-cell lymphoma. Axial bone CT image (A) shows a right frontal sinus mass (thin white arrow) with destruction of the anterior sinus wall (open arrow). Axial STIR MRI image (B) shows a homogeneous intermediate-to-low intensity mass with extension into the frontal soft tissue (thin white arrow). Diffuse homogeneous enhancement is seen within the mass on axial postcontrast T1W image (C) marked by thin white arrows. Bone destruction is seen (open arrow). Axial DWI MRI image (D) shows restricted diffusion within the mass (open arrow) indicative of cellular nature. Low T2-signal intensity and restricted diffusion in this mass are suggestive of lymphoma.

origin and peak incidence is in the fifth decade. Characteristic high T2W signal intensity is seen on MRI, T1W signal intensity is low and there is avid post contrast enhancement. Intratumoral calcifications are common.[7,20,25]

Synovial sarcomas have received more attention on the current WHO classification, and is included in the SN tumors predominantly as a differential diagnostic consideration for BSNS (described later in the new/emerging entities). These tumors are common at the skull base.

SN Metastasis

Metastatic lesions to the SN region are rare but not unknown.[34] Maxillary sinus is the most commonly involved and the common primary tumors are breast, lung, thyroid, kidney, and prostate. The symptoms are similar to primary tumors of the SN region. Prognosis is poor due to the common coexistent disseminated disease.

New/Emerging SN Neoplasms

NUT Carcinoma

NUT carcinoma is a newly described rare entity in SN neoplasms which derives its name from nuclear protein in testis (NUTM1) gene. There is rearrangement of NUTM1 gene on chromosome 15q14 in NUT carcinoma and the diagnosis depends on demonstrating this rearrangement. The most common partner gene is BRD4 on chromosome 19. The tumor is also called the NUT midline carcinoma and was initially described in the mediastinum. It is most common in children and young adults and is slightly more common in females, but all ages may be affected. Most head and neck NUT carcinomas arise in the nasal cavity and paranasal sinuses. These are high-grade poorly differentiated tumors with evidence of squamous differentiation where keratinized squamous cells may be occasionally seen abruptly juxtaposed to the undifferentiated component. Round-blue cell morphology is seen with SNEC, SNUC, ENB, and SCC in the differential diagnosis.[18,32,35]

On imaging, the tumor has an aggressive infiltrating appearance with frequent bone destruction and orbital and intracranial extension (Fig. 13). The tumor is heterogeneous and enhances avidly on contrast administration on both CT and MRI. Tumor necrosis and necrotic lymphadenopathy are common. Necrosis may be better delineated on MRI. Multi-modality tumor mapping including FDG-PET helps in characterizing the primary lesion, identifying nodal disease and excluding distant metastasis. The tumor carries a poor prognosis. Lymph node and/or distant metastasis are common and can be seen in about half the cases.[18,32,35]

Correct diagnosis of NUT carcinoma allows these patients to be enrolled in international NUT midline carcinoma registry. SN carcinomas with an undifferentiated component should therefore be tested for NUT rearrangement to direct these patients to focused trials.

Respiratory Epithelial Lesions: Respiratory Epithelial Adenomatoid Hamartoma and Seromucinous Hamartoma

Two rare benign entities are included in the group with the heading of respiratory epithelial lesions – Respiratory epithelial adenomatoid hamartoma (REAH) and seromucinous hamartoma (SH). The 2 lesions likely represent a spectrum of a similar process. Adults are mostly affected, and posterior nasal septum, in the region of the olfactory cleft is the predominant site of origin. Recurrence is uncommon and metastasis is rarely seen.[18,36]

On a microscopic level, gland-like structures arise in continuity with the surface epithelium, lined by multilayered ciliated respiratory epithelium with a frequent inflammatory background and occasional squamous or cartilaginous metaplasia in REAH. These lesions are homogeneously hypodense on CT (Fig. 14) commonly associated with enlargement of the olfactory cleft, without bone destruction. On MRI, uniformly enhancing well-defined tissue is seen.

SH differs from REAH histologically in that the predominant underlying glandular component in SH consists of seromucous glands that are typically immunoreactive with antibodies to S100 protein. The larger glands of REAH are nonreactive to S100. SH has a female predilection and is seen in middle age. Unilateral nasal obstruction is the most common presenting symptom. Posterior nasal septum is a common site of origin. On imaging REAH and SH are often indistinguishable and present as nasal septal homogeneous polypoid masses.[18,36] Proteinaceous content due to increased glandular activity can give a high signal on noncontrast T1W images. Differential

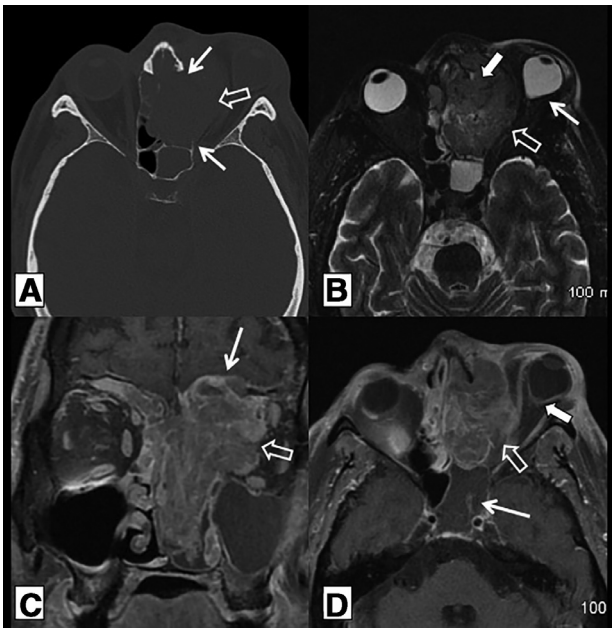

Figure 13 NUT carcinoma. Axial bone CT image (A) shows a large mass within the left nasal cavity with surrounding bone destruction (small white arrows). There is extension into the left orbit (open arrow). Axial STIR MRI image (B) shows a lobulated mass with intermediate-to-low signal intensity suggestive of hypercellular nature (thick white arrow). Intraorbital extension is seen with displacement of the orbital structures (open arrow). There is marked proptosis causing stretching of the optic-nerve-sheath complex and tenting of the globe (thin white arrow). Coronal postcontrast T1W MRI image (C) shows the large infiltrating destructive mass with intraorbital (open arrow) and intracranial (thin white arrow) extension. NUT carcinomas are notorious for this and for frequent nodal and distant metastasis. Axial postcontrast T1W MRI image (D) shows the infiltrating mass (open arrow) with left-sided proptosis (thick arrow). Homogeneous low intensity contents with thin mucosal lining in the left sphenoid sinus represent retained secretions (thin white arrow).

considerations include the common inflammatory polyps and REAH. Surgical removal is curative and recurrence is rare.

Chondromesenchymal Hamartoma

CMH has been known as a distinct entity for a while but has been included in the WHO classification only recently.[1] It is a rare benign lesion which originates in the nasal cavity and paranasal sinuses and is usually seen in infants. CMH is associated with pleuropulmonary blastoma tumor predisposition disorder, which is due to germline or somatic mutations of the DICER gene.[37-39] Although it is a benign entity, the imaging features are those of an aggressive lesion with infiltrative margins and bone erosion. Intracranial and intraorbital extension has been described. The tumors are heterogeneous with frequent cystic areas and calcification. Enhancement depends on the prevailing component and may be moderate if the solid component predominates. Differential diagnosis includes hemangioma, IP, ossifying fibroma, etc, although the avid enhancement usually associated with hemangiomas and IPs is not usually seen in CMH.[37-39]

Surgical excision is the treatment if choice although clear surgical margins are difficult to obtain due to the infiltrative nature. Recurrence is therefore common. Malignant transformation is possible but rare.

Biphenotypic SN Sarcoma

The histological features of this tumor have been noticed in the past and it is thought that it may have been misdiagnosed as cellular schwannoma, malignant nerve sheath tumor, or synovial sarcoma. It was initially described as "low-grade SN sarcoma with neural and myogenic differentiation" and the histopathology is that of an infiltrative proliferation of spindle cells arranged in fascicles entrapping downward extensions of hyperplastic respiratory surface epithelium, with occasional hemangiopericytoma-like vascular pattern and focal rhabdomyoblastic

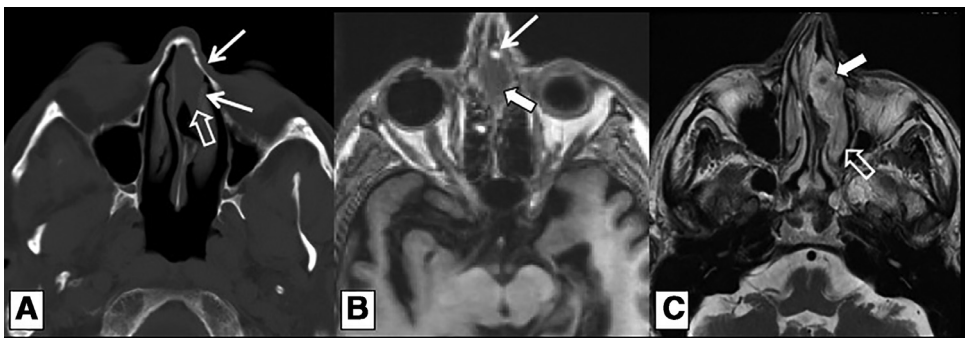

Figure 14 Respiratory epithelial adenomatoid hamartoma (REAH). Axial bone CT image (A) shows a polypoid soft tissue mass in the left nasal cavity (open arrow). The adjacent bones are unremarkable without erosion (thin white arrows). Axial noncontrast T1W MRI image (B) shows a low intensity left nasal cavity polypoid mass (thick white arrow). A small well-defined area of high T1W intensity (thin white arrow) likely represents internal proteinaceous component due to glandular activity. Proteinaceous areas are much more common in seromucinous hamartomas (SH), although REAH and SH may at times be indistinguishable on imaging. Axial T2W MRI image (C) shows the hyperintense mass, with a few cystic areas (thick white arrow) due to glandular activity. Attachment to the inferior turbinate is shown (open arrow). Note that the signal characteristics of the lesion are not very different from normal nasal mucosa.

differentiation. PAX3-MAML3 gene fusion is the distinctive immunohistochemical and molecular feature.[3,25]

BSNS tends to arise in middle-aged women with a 2:1 female to male ratio and has a predilection for superior aspects of the nasal cavity and ethmoids. On imaging, these tumors are expansile and locally destructive. Areas of internal calcification are seen and there is avid postcontrast enhancement (Fig. 15). Approximately half of these tumors recur but distant metastasis is not yet known.[3,25]

SMARCB1 (INI-1) Deficient Carcinoma

SMARCB1 is a tumor suppressor gene located on chromosome 22, which is universally expressed in all normal tissues. The inactivation of this gene leads to the development of various malignant neoplasms that tend to share rhabdoid cytomorphology. This group of tumors also includes the atypical teratoid/rhabdoid tumors of the CNS, renal medullary carcinoma, and epithelioid malignant peripheral nerve sheath tumors. At this time, it remains unclear however, whether SMARCB1 deficient carcinoma is a distinct entity or rather a pattern that can be seen in a variety of tumor types.[33,40,41] The tumors test negative for HPV and NUT. Histological differential diagnosis includes nonkeratinizing SCC, SNUC, NUT carcinoma, and melanoma.

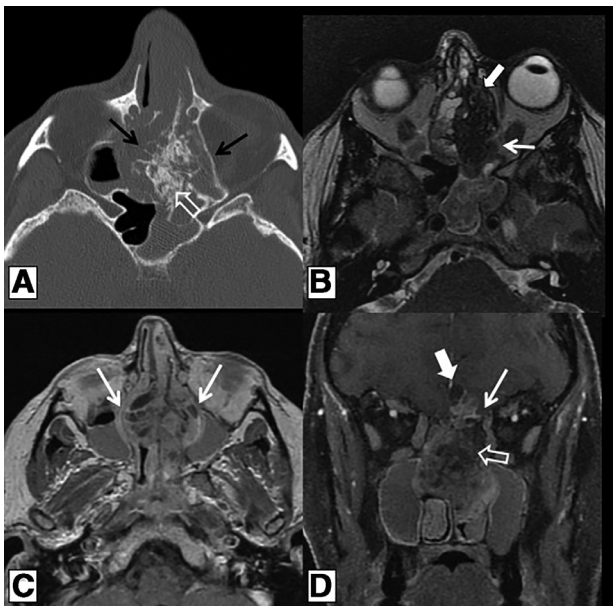

Figure 15 Biphenotypic sinonasal sarcoma. Axial bone CT image (A) demonstrating a heterogeneous mass in the superior nasal cavity (thin black arrows) with large areas of calcification (open arrow). The tumor is destructive and crosses the midline. Nasal cavity is a common location. Axial STIR MRI image (B) shows large low intensity areas corresponding to areas of calcification (thick white arrow). There is destruction of the left orbital medial wall (thin white arrow). Axial postcontrast T1W MRI image (C) shows the heterogeneous nature of the mass (thin white arrows) due to the mixed tissue components. Coronal postcontrast T1W MRI image shows the locally destructive nature of the lesion with erosion of the anterior skull base (thin white arrow) and intracranial extension (thick white arrow). Low intensity nonenhancing areas (open arrow) are due to calcific components.

Of the reported cases, a wide age range has been observed from 19 years to 89 years. More males have been reported than females. Ethmoid sinuses have been affected most commonly with frequent involvement of the nasal cavities. The tumors have an aggressive infiltrative appearance with frequent bone erosion (Fig. 16) and intracranial/intraorbital extension. Tumor necrosis is common and peritumoral cysts may be seen. Heterogeneous and avid postcontrast enhancement is seen. Regional lymphadenopathy and distant metastasis have been documented in a small number of the reported cases. Recurrence has been reported in approximately half the cases. A 50% mortality rate has been described.[33,39,40]

HPV-related SN Carcinoma

The new WHO classification has separated the HPV-related oropharyngeal cancers due to the high prevalence of HPV positivity in neoplasms of the oropharynx and due to their clinical and histological distinctness. In order of prevalence, SN tract is the second most common site to harbor HPV, after the oropharynx, although the favorable prognosis associated with HPV positive oropharyngeal SCC has not been observed with HPV-related carcinomas of the SN tract. Most HPV-related SN carcinomas are nonkeratinizing SCCs. The different histological variants seen with HPV-related oropharyngeal SCCs are also seen with HPV-related carcinomas of the SN tract, with the exception of one variant referred to as "SN HPV-related carcinoma with adenoid cystic-like features," which is only described in the SN tract. Since the recognition of this tumor entity, several cases have been reported and as more information accumulated, there has been greater appreciation of the full morphologic spectrum of this tumor. A new name has therefore been assigned to this entity and the term now includes a broader histological spectrum. This entity now called the "HPV-related multiphenotypic SN carcinoma" demonstrates differentiation along multiple cell lines with features consisting of highly cellular proliferations of basaloid cells, lobules and cribriform nests reminiscent of ACC, squamous dysplasia of the surface epithelium and less frequently squamous differentiation with keratin production, bizarre pleomorphism, sarcomatoid transformation, and cartilaginous differentiation.[42-44] High-grade features are seen and perineural invasion is uncommon. This entity has been found more commonly in females and is seen between the ages of 40 and 75 years. Most tumors affect the nasal cavity with or without sinus involvement. Late recurrence is not uncommon and distant metastasis has been reported.[42-44]

Renal Cell-like Adenocarcinoma

Renal cell-like adenocarcinoma is an uncommon entity defined by its histologic similarity to clear cell renal carcinoma. The tumor may be difficult to differentiate from metastatic RCC; however, it is negative for immunohistochemical markers like PAX8, RCC, and vimentin in contrast to the metastatic RCC. The tumor has been reported slightly more commonly in females and a wide age range has been observed ranging from 22 to 77 years. The tumor is indolent and metastatic disease and recurrence has not been reported in the few known cases.[1,3]

Figure 16 SMARCB1 deficient carcinoma. Axial postcontrast soft tissue CT image (A) shows an avidly enhancing mass (thin arrows). Destructive appearance with erosion of the turbinates and extension to the right maxillary ostium (open arrow) is noted on coronal postcontrast soft tissue CT image (B). Coronal bone CT image (C) clearly shows the destruction of turbinates and osseous structures at the maxillary ostium. These tumors are highly aggressive with frequent intracranial extension and peritumoral cysts.

Summary

Several new entities have been added in the new 2017 WHO classification of SN tumors. While it is important to keep abreast of the latest tumor types to ensure accurate diagnosis, optimal treatment and correct prognostication, the primary role of imaging remains differentiation of malignant neoplasms from benign processes; and tumor mapping. Multiplanar MRI with contrast is of greatest value in tumor detection, differentiation, and delineation of extent. Perineural tumor spread and bone marrow infiltration are also better discerned on MRI. CT can identify bone erosion more accurately and FDG-PET is highly useful for discovering distant metastasis. Differentiating malignant SN tumors can be challenging but mindfulness of specific features such as cysts at the tumor-brain interface for ENB, T1W hyperintense signal characteristic of melanoma and hypercellular nature of lymphoma; can aid in diagnosis.

Key Points

1. Differentiation of benign SN processes from malignant lesions is important. An enlarging SN "polyp" is probably not benign. Closer look at the surrounding structures, adjacent bone; and evaluation with further imaging may be revealing.
2. Making a pathological diagnosis is not possible in all cases. Describe tumor size, extent, and involvement of the surrounding structures. Look for perineural tumor spread and nodal metastasis.
3. Be aware of the new and emerging entities. Gene testing may make specific diagnosis and help in targeted treatment.
4. Metastatic lesions are rare but not unknown in the SN region. Clinical notes and previous imaging are waiting to be explored.

References

1. Thompson LDR, Franchi A: New tumor entities in the 4th edition of the World Health Organization classification of head and neck tumors: Nasal cavity, paranasal sinuses and skull base. Virchows Arch 472:315-330, 2018
2. Stelow EB, Bishop JA: Update from the 4th edition of the World Health Organization Classification of Head and Neck Tumours: Tumors of the nasal cavity, paranasal sinuses and skull base. Head Neck Pathol 11:3-15, 2017
3. Bishop JA: Newly described tumor entities in sinonasal tract pathology. Head Neck Pathol 10:23-31, 2016
4. Koeller KK: Radiologic features of sinonasal tumors. Head Neck Pathol 10:1-12, 2016
5. Madani G, Beale TJ, Lund VJ: Imaging of sinonasal tumors. Semin Ultrasound CT MRI 30:25-38, 2009
6. Som PM, et al: Tumors and tumor-like conditions of the sinonasal cavities. Head and Neck Imaging 2011253-410, 2011
7. Harvey RJ, Dalgorf DM: Sinonasal malignancies. Am J Rhinol Allergy 27 (3_suppl):S35-S38, 2013
8. Naval Baudin P, Pons Escoda A, Cos Domingo M, et al: Invasive Sinonasal Lesions: From the Nasal Fossa and Paranasal Sinuses to the Endocranium. Curr Probl Diagn Radiol 47:168-178, 2018
9. Ozturk K, Gawande R, Gencturk M, et al: Imaging features of sinonasal tumors on positron emission tomography and magnetic resonance imaging including diffusion weighted imaging: A pictorial review. Clin Imaging 51:217-228, 2018. https://doi.org/10.1016/j.clinimag.2018.05.018
10. Kim SH, Mun SJ, Kim HJ, et al: Differential Diagnosis of Sinonasal Lymphoma and Squamous Cell Carcinoma on CT, MRI, and PET/CT. Otolaryngol Head Neck Surg 159:494-500, 2018
11. Munhoz L, Abdala Junior R, Abdala R, Arita ES: Diffusion-weighted magnetic resonance imaging of the paranasal sinuses: A systematic review. Oral Surg Oral Med Oral Pathol Oral Radiol 126:521-536, 2018
12. Wang XY, Yan F, Hao H, et al: Improved performance in differentiating benign from malignant sinonasal tumors using diffusion-weighted combined with dynamic contrast-enhanced magnetic resonance imaging. Chin Med J (Engl) 128(5):586-592, 2015
13. El-Gerby KM, El-Anwar MW: Differentiating benign from malignant sinonasal lesions:Feasibility of diffusion weighted MRI. Int Arch Otorhinolaryngol 21:358-365, 2017
14. Fujima N, Sakashita T, Homma A, et al: Advanced diffusion models in head and neck squamous cell carcinoma patients: Goodness of fit, relationships

among diffusion parameters and comparison with dynamic contrast-enhanced perfusion. Magn Reson Imaging 36:16-23, 2017
15. Wang F, Sha Y, Zhao M, et al: High-Resolution Diffusion-Weighted Imaging Improves the Diagnostic Accuracy of Dynamic Contrast-Enhanced Sinonasal Magnetic Resonance Imaging. J Comput Assist Tomogr 41:199-205, 2017
16. Wang X, Zhang Z, Chen Q: Effectiveness of 3 T PROPELLER DUO diffusion-weighted MRI in differentiating sinonasal lymphomas and carcinomas. Clin Radiol 69:1149-1156, 2014
17. Kitamoto E, Chikui T, Kawano S, et al: The application of dynamic contrast-enhanced MRI and diffusion-weighted MRI in patients with maxillofacial tumors. Acad Radiol 22:210-216, 2015
18. Dean K, Shatzkes D, Phillips CD, New and emerging sinonasal tumor and tumor like entities, in ASHNR Annual Meeting. Savannah.
19. Hennessey PT, Reh DD: Benign sinonasal neoplasms. Am J Rhinol Allergy 27(3_suppl):S31-S34, 2013
20. McCollister KB, Hopper BD, Michel MA: Sinonasal neoplasms: Update on classification, imaging features, and management. Appl Radiol 44 (12):7-15, 2015
21. Eller R, Sillers M: Common fibro-osseous lesions of the paranasal sinuses. Otolaryngol Clin N Am 39:585-600, 2006
22. Eversole R, Su L, ElMofty S: Benign fibro-osseous lesions of the craniofacial complex. A review. Head Neck Pathol 2:177-202, 2008
23. Agarwal M, Michel MA: Sino-orbital pathologies: An approach to diagnosis and indentifying complications. Appl Radiol 46(8):8-20, 2017
24. Salina ACI, Souza PMM, Gadelha, et al: Ossifying fibroma: an uncommon differential diagnosis for T2-hypointense sinonasal masses. Radiol Case Rep 12(2):313-317, 2017. https://doi.org/10.1016/j.radcr.2017.03.019
25. Purgina B, Lai CK: Distinctive head and neck bone and soft tissue neoplasms. Surg Pathol Clin 10:223-279, 2017
26. Yang BT, Wang ZC, Xian JF, et al: Leiomyoma of the sinonasal cavity: CT and MRI findings. Clin Radiol 64:1203-1209, 2009
27. Riley CA, Marino MJ, Hawkey N, et al: Sinonasal Tract Inflammation as a Precursor to Nasopharyngeal Carcinoma: A Systematic Review and Meta-Analysis. Otolaryngol Head Neck Surg 154:810-816, 2016
28. Wu EL, Riley CA, Hsieh MC, et al: Chronic sinonasal tract inflammation as a precursor to nasopharyngeal carcinoma and sinonasal malignancy in the United States. Int Forum Allergy Rhinol 7:786-793, 2017
29. Badger D, Aygun N: Imaging of perineural spread in head and neck cancer. Radiol Clin N Am 55:139-149, 2017
30. Barrett AW, Speight PM: Perineural invasion in adenoid cystic carcinoma of the salivary glands: A valid prognostic indicator? Oral Oncol 45:936-940, 2009
31. Ginsberg LE: Perineural Tumor spread associated with head and neck malignancies. Head and Neck Imaging 20111021-1049, 2011
32. Kakkar A, Antony VM, Irugu DVK, et al: NUT midline carcinoma: A series of five cases, including one with unusual clinical course. Head Neck Pathol 12:230-236, 2018
33. Agaimy A, Hartmann A, Antonescu CR: SMARCB1 (INI-1)-deficient Sinonasal Carcinoma: A Series of 39 Cases Expanding the Morphologic and Clinicopathologic Spectrum of a Recently Described Entity. Am J Surg Pathol 41:458-471, 2017
34. Lopez F, Devaney KO, Hanna EY, et al: Metastases to nasal cavity and paranasal sinuses. Head Neck 38:1847-1854, 2016
35. Shaikh F, Pagedar N, Awan O, et al: Sinonasal NUT-Midline Carcinoma - A Multimodality Approach to Diagnosis. Staging and Post-Surgical Restaging. Cureus 7:e288, 2015
36. Huang CC, Lee TJ, Huang CC, et al: Seromucinous hamartoma in the nasal cavity medial to the middle turbinate: report of 2 cases and review of the literature. Head Neck 37:E15-E18, 2015
37. wang T, Li W, Wu X, et al: Nasal Chondromesenchymal hamartoma in young children: CT and MRI findings and review of literature. World J Surg Oncol: 1-5, 2014. 12/1/257
38. Unal A, Kum RO, Avci Y, et al: Nasal chondromesenchymal hamartoma, a rare pediatric tumor: case report. Turk J Pediatr 58:208-211, 2016
39. Yao-Lee A, Ryan M, Rajaram V: Nasal chondromesenchymal hamartoma: Correlation of typical MR, CT and pathological findings. Pediatr Radiol 41:675-677, 2011
40. Bishop JA, Antonescu CR, Westra WH: SMARCB1 (INI-1)-deficient carcinomas of the sinonasal tract. Am J Surg Pathol 38:1282-1289, 2014
41. Shatzkes DR, Ginsberg LE, Wong M, et al: Imaging Appearance of SMARCB1 (INI1)-Deficient Sinonasal Carcinoma: A Newly Described Sinonasal Malignancy. AJNR Am J Neuroradiol 37:1925-1929, 2016
42. J.A. Bishop, S. Andreasen, J.F. Hang, et al, HPV-related Multiphenotypic Sinonasal Carcinoma An Expanded Series of 49 Cases of the Tumor Formerly Known as HPVrelated Carcinoma With Adenoid Cystic Carcinoma-like Features. Am J Surg Pathol, 41, 1690-1701.
43. Adamane SA, Mittal N, Teni T, et al: Human papillomavirus-related multiphenotypic sinonasal carcinoma with unique HPV type 52 association: A case report with review of literature. Head Neck Pathol 2018. [Epub ahead of print]
44. Bishop JA, Westra WH: Human papillomavirus-related multiphenotypic sinonasal carcinoma: An emerging tumor type with a unique microscopic appearance and a paradoxical clinical behaviour. Oral Oncol 87:17-20, 2018